nature COMMUNICATIONS

ARTICLE

Received 11 Jul 2014 | Accepted 7 Nov 2014 | Published 22 Jan 2015

DOI: 10.1038/ncomms6779

Autophagy enhances NFκB activity in specific tissue macrophages by sequestering A20 to boost antifungal immunity

Masashi Kanayama[1], Makoto Inoue[1], Keiko Danzaki[1], Gianna Hammer[1], You-Wen He[1] & Mari L. Shinohara[1,2]

Immune responses must be well restrained in a steady state to avoid excessive inflammation. However, such restraints are quickly removed to exert antimicrobial responses. Here we report a role of autophagy in an early host antifungal response by enhancing NFκB activity through A20 sequestration. Enhancement of NFκB activation is achieved by autophagic depletion of A20, an NFκB inhibitor, in F4/80^{hi} macrophages in the spleen, peritoneum and kidney. We show that p62, an autophagic adaptor protein, captures A20 to sequester it in the autophagosome. This allows the macrophages to release chemokines to recruit neutrophils. Indeed, mice lacking autophagy in myeloid cells show higher susceptibility to *Candida albicans* infection due to impairment in neutrophil recruitment. Thus, at least in the specific aforementioned tissues, autophagy appears to break A20-dependent suppression in F4/80^{hi} macrophages, which express abundant A20 and contribute to the initiation of efficient innate immune responses.

[1] Department of Immunology, Duke University Medical Center, Durham, North Carolina 27710, USA. [2] Department of Molecular Genetics and Microbiology, Duke University Medical Center, Durham, North Carolina 27710, USA. Correspondence and requests for materials should be addressed to M.L.S. (email: mari.shinohara@duke.edu).

Autophagy is a highly conserved cellular process in eukaryotes, and is induced by various pathogen-associated molecular patterns and cytokines to eliminate intracellular microbes through autophagosomal digestion in mammals[1–3]. Autophagy can unselectively eliminate cytoplasmic proteins and organelles, and contributes to amino-acid recycling within a cell. At the same time, selective degradation of particular proteins is mediated by autophagy adaptor proteins such as p62, also called sequestosome-1, which contributes to maintenance of cellular activity. Recent studies have shown that autophagy eliminates assembled inflammasomes in macrophages[4] and BCL10 to limit T-cell receptor signalling in T cells[5], both resulting in downregulation of immune responses. Thus, autophagy is currently known to suppress immune responses to protect hosts from possible collateral damage caused by overly active immunity[6].

It is reported that dectin-1, a fungal cell wall component β-glucan receptor, triggers conversion of microtubule-associated protein 1 light chain 3 (LC3)-I to LC3-II (ref. 7), which is used to monitor autophagy. A recent report demonstrated a protective role of autophagy in *Candida* infection[8], while others showed that autophagy is not critical for host protection against *C. albicans*[9,10]. Thus, the specific role(s) of autophagy during *Candida* infection may be considered controversial.

Various cell types in the host immune system play a protective role against *Candida* infection. For example, neutrophils prevent fungal growth and invasion, particularly at the early stage of infection. Therefore, neutropenia is a major causal factor in disseminated candidiasis[11,12]. Neutrophils prevent *Candida* hyphal formation by phagocytosed conidia, although macrophages are destroyed by germinated hyphae of ingested *Candida*[13]. As a result, neutrophils are viewed as critical cells for the host's protection against *Candida* infection. Because of their short life span (half-life of ∼6 h in circulation[14]), prompt recruitment of neutrophils from bone marrow (BM) is critical for host protection. On the other hand, tissue-resident macrophages are considered to be an important source of neutrophil chemoattractants; thus, deletion of tissue-resident macrophages results in the failure of neutrophil recruitment and neutrophil-dependent immune responses[15–17]. F4/80^{hi} macrophages are largely tissue-resident[18–21], although it is possible that F4/80^{hi} macrophages from different organs have tissue-specific phenotypes. In contrast, as previously demonstrated with BM chimera mice, 95–100% of F4/80^{lo} macrophages in various organs are replaced by donor BM cells[20]. It is also known that, during infection, F4/80^{lo} monocytes/macrophages are recruited in the infected sites[22,23], while the spleen has a number of monocytes even in naive mice. Distinct gene expression pattern between F4/80^{lo} and F4/80^{hi} macrophages[20] suggests different functions between the two populations. Currently, it is unknown which macrophage subset is the main producer of neutrophil chemoattractants in fungal infection.

Host cells are equipped with various mechanisms that negatively regulate immune responses to avoid hyperinflammation and autoimmunity. For example, A20 acts as a pivotal NFκB suppressor under Toll-like receptors (TLRs), and tumour necrosis factor receptor (TNFR)[24]. A20 deficiency causes severe autoimmune inflammation by excessive NFκB activation[25–27]. However, such a negative regulatory system, if sustained, hampers host immune responses to act quickly on the clearance of pathogens. In order to solve this dilemma, immune suppression by A20 must be strictly controlled when infections occur. Therefore, timely downregulation of A20 is considered to be important during acute infections. Although NFκB is known to induce A20 expression[28], the mechanism underlying the negative regulation of A20 is not clear.

In the current study, we evaluate antifungal immunity in mice conditionally lacking autophagy-related protein-7 (ATG7), essential for autophagosome formation[29] and LC3-associated phagocytosis[30], in myeloid cells. Our data demonstrate that autophagy downregulates A20 in F4/80^{hi} macrophages through p62-associated autophagic sequestration and that the resulting NFκB activation induces expression of chemokines at an early stage of *Candida* infection. On the basis of these results, we suggest a mechanism by which autophagy protects hosts by enhancing NFκB signalling in tissue-resident macrophages, which indeed play a sentinel role at the early stage of fungal infections.

Results

Lack of ATG7 attenuates host resistance against *Candida*. To assess the impact of ATG7 on fungal immunity, we generated *Atg7*$^{fl/fl}$*lysozyme M* (*LysM*)$^{cre/+}$ mice (denoted as '*Atg7* CKO mice' hereafter), in which myeloid cells, such as macrophages, dendritic cells (DCs) and neutrophils, lack autophagy. We confirmed that *Atg7* mRNA expression was abolished in peritoneal macrophages (Supplementary Fig. 1). When the mice were intravenously injected with either 10^6 (Fig. 1a,b) or 2×10^5 (Fig. 1c,d) conidia of *Candida*, weights and the survival of *Atg7* CKO mice were significantly reduced compared with control *LysM*$^{cre/+}$ mice (denoted as 'WT mice' hereafter). Importantly, the significant difference in weight reduction was observed on day 1 or 2 (Fig. 1b,d). Therefore, the impact of autophagy in myeloid cells on host protection was apparent at a very early stage (24–48 h) of fungal infection. We next compared fungal burdens in WT and *Atg7* CKO mice in the kidney and spleen on day 3. Fungal loads in both organs were significantly increased in *Atg7* CKO mice (Fig. 1e), and the increased fungal load was also histologically identified in the kidney (Fig. 1f).

ATG7 has no direct influence on fungal killing. In an effort to describe the protection mechanism of autophagy in innate immune responses against fungal pathogen, we first examined whether or not *Candida* could induce autophagy in innate immune cells. Macrophage cell line (RAW-Blue cell) was cocultured with *Candida* conidia, and the induction of autophagy was evaluated by detecting LC3 puncta formation and LC3-II induction. Sixty minutes after the stimulation with conidia, LC3 puncta formation was clearly observed (Fig. 2a). Immunoblotting data also confirmed the induction of autophagy as quickly as 5 min following the coculture set-up (Fig. 2b). Autophagy is known to enhance phagocytosis of viral, bacterial and parasitic pathogens[1–3]. We thus next examined whether or not ATG7-mediated phagocytic activity in macrophages and neutrophils. The phagocytic capacity of both bone marrow-derived macrophages (BMDMs) and neutrophils, obtained from *Atg7* CKO and WT mice, was assessed with flow cytometry. Unexpectedly, the absence of autophagy did not affect the percentages of host cells showing a fluorescent marker for *Candida* (Fig. 2c,d) and phagocytic index (the number of *Candida* detected with single macrophages; Fig. 2e). No change in *Atg7* CKO was found also in thioglycollate-elicited peritoneal and total splenic macrophages (Supplementary Fig. 2).

Because flow cytometry does not distinguish *Candida*-engulfed host cells from those simply attaching to *Candida*, we eye-counted *Candida*-engulfed macrophages from at least 100 cells randomly captured with confocal microscopic images. The results also indicated that WT and *Atg7* CKO macrophages had similar abilities to phagocytose *Candida* (Supplementary Fig. 3). In addition, the generation of reactive oxygen species, toxic for ingested microbes including *Candida*, was also unaltered in

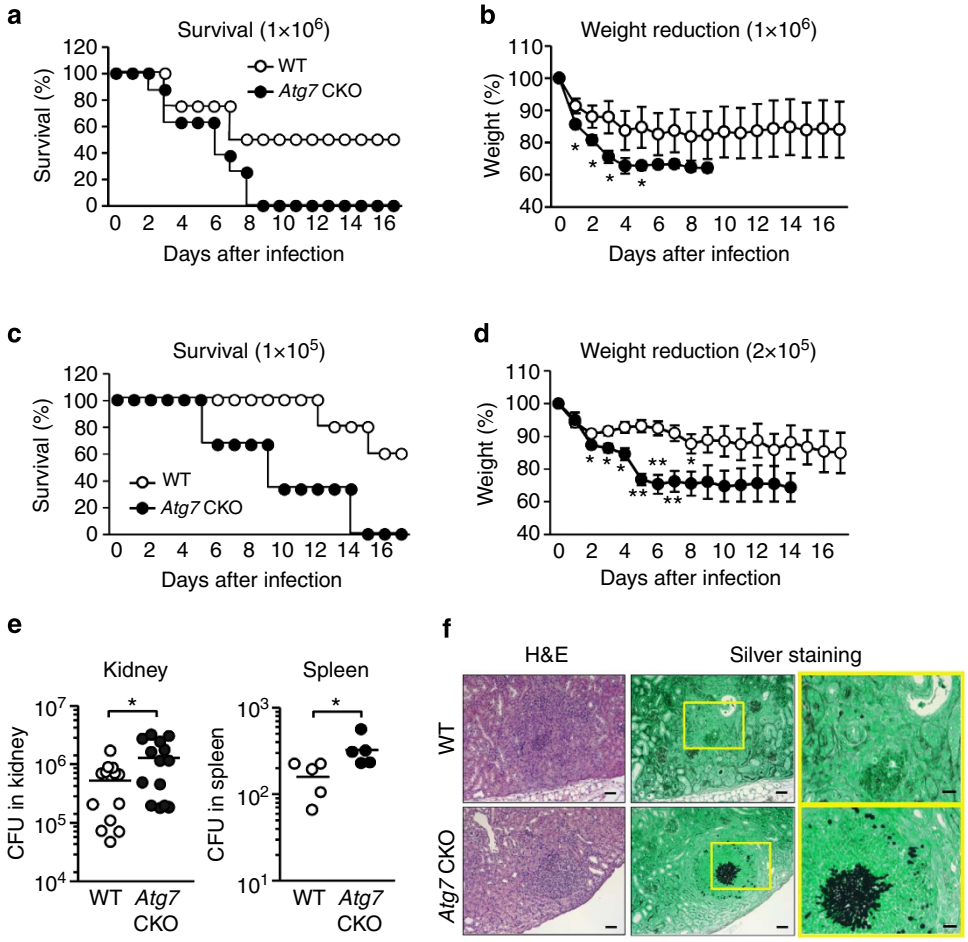

Figure 1 | Absence of ATG7 in myeloid cells decreases host resistance against *Candida* infection. (**a**–**d**) $Atg7^{fl/fl}LysM^{cre/+}$ (*Atg7* CKO) and $LysM^{cre/+}$ (WT) mice were systemically infected by *i.v.* injection of *C. albicans*. Mouse survival (**a**,**c**) and weight (**b**,**d**) were monitored. Innocula of *Candida* were 10^6 spores per mouse to *Atg7* CKO ($n=9$) and WT ($n=12$; **a**,**b**), and 2×10^5 spores per mouse to *Atg7* CKO ($n=12$) and WT($n=10$; **c**,**d**). (**e**) Fungal burdens in the kidney and the spleen of *Atg7* CKO and WT mice 3 days after 10^6 *C. albicans i.v.* injection. One circle denotes a result from one mouse. (**f**) Haematoxylin and eosine and silver staining of sections from kidneys of WT and *Atg7* CKO mice 3 days after 10^6 *C. albicans i.v.* injection. *Candida* is observed with black in silver staining. Magnified views of the panels in the middle (yellow rectangles) are shown on the right. Scale bars in the left and middle panels indicate 200 μm; and scale bars in the panels on the right indicate 60 μm. Data are representative of independent two experiments. Error bars represent mean ± s.d. Student's *t*-test was used for statistical analysis. $^*P<0.05$, $^{**}P<0.01$.

Atg7-deficient macrophages (Fig. 2f). Our *ex vivo* assay to evaluate host cell inhibition of *Candida* growth showed comparable results between WT and *Atg7* CKO with BMDMs, thioglycollate-elicited peritoneal macrophages, total splenic macrophages and neutrophils (Fig. 2g–i; Supplementary Fig. 2b,d). These results suggested that ATG7 likely does not play a role either in host cell-intrinsic functions to phagocytose, or in inhibiting expansion of *Candida* both in macrophages and neutrophils. This is in clear contrast to the role of autophagy in infections by viruses, bacteria and parasites.

We then tried to evaluate the time course of live *Candida* engulfment in macrophages, particularly within LC3 cargos. A few conidia were phagocytosed at 5 and 10 min, and we could not evaluate the presence of *Candida*-containing LC3 cargos. Yet, complete phagocytosis of conidia was observed at 30, 45 and 60 min (Supplementary Fig. 4a). Unexpectedly, no conidia were found within LC3 cargos, but LC3 protein was rather randomly distributed (Fig. 2j; Supplementary Fig. 4a; Supplementary Table 1). Spores contained within LC3 cargos were sought in at least 100 macrophages at each time point; however, we found no spores contained in LC3 cargos. As a positive control, we could confirm LC3 recruitment to zymosan particles (Supplementary Fig. 4b,c; Supplementary Table 1), as previously reported[7]. These data suggest that live *Candida* was not cleared in autophagosomes, and this is also a clear contrast to the role of autophagy against viruses, bacteria and parasites.

Autophagy increases neutrophil recruitment. *Atg7* CKO mice showed severe weight reduction as early as day 1 (Fig. 1b). As neutrophils are responsible for *Candida* clearance at the early stage of infection[12,31], we investigated whether the lack of autophagy affected neutrophil recruitment to the kidney and spleen at 4 and 24 h post infection (hpi). The 4-h time point was too early to statistically evaluate neutrophil infiltration; however, the result at 24 hpi using WT mice showed a sizeable increase in numbers of neutrophils (Supplementary Fig. 5). At 24 hpi, the cellularity of total splenocytes in *Atg7* CKO mice was comparable to that in WT mice (Supplementary Fig. 6a); however, *Atg7* CKO mice showed significantly reduced neutrophil recruitment in both the kidney and spleen (Fig. 3a,b). Interestingly, WT mice showed a more drastic decrease in BM neutrophil population at 24 hpi than did *Atg7* CKO mice after infection (Fig. 3c), while WT and *Atg7* CKO naive mice had similar sizes of the BM neutrophil

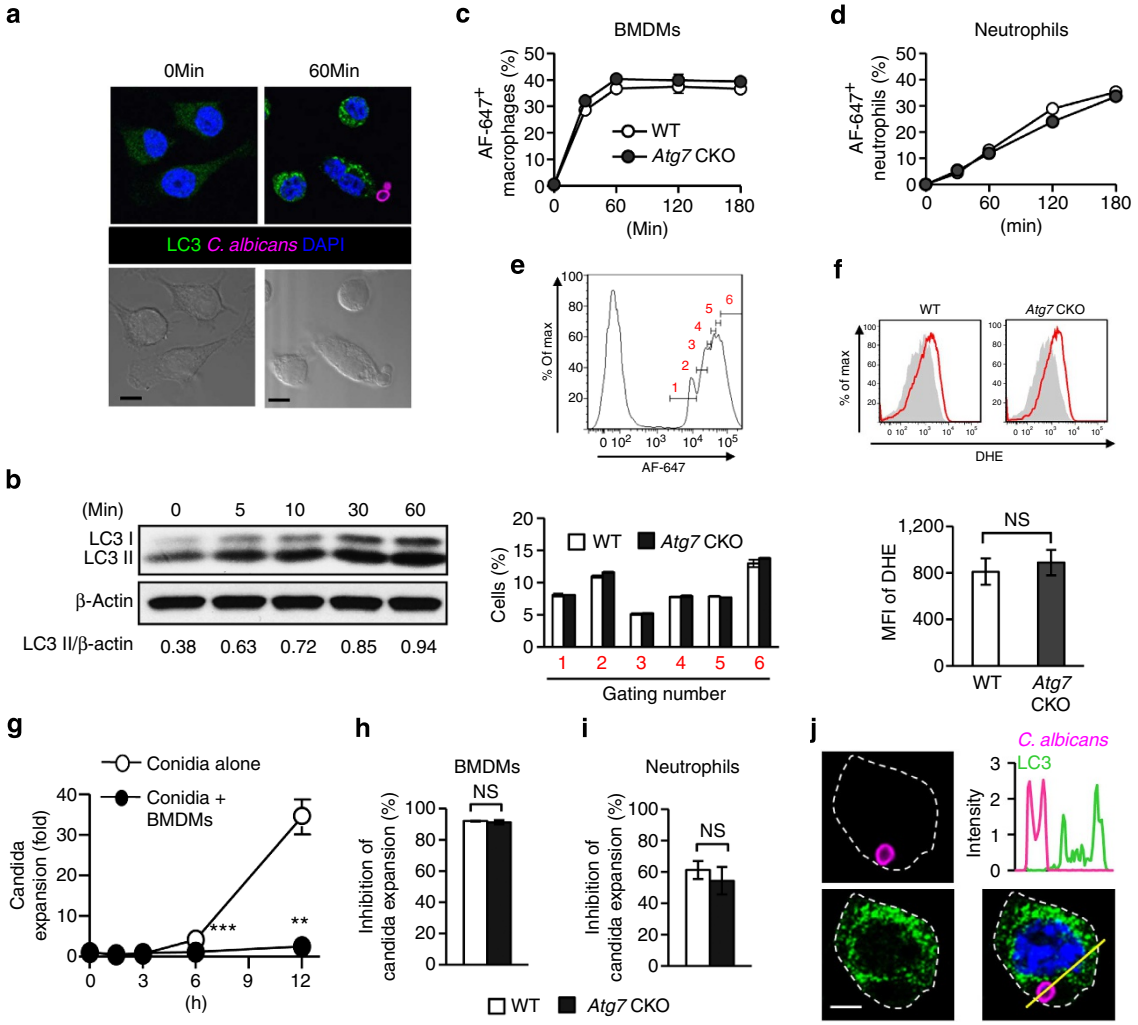

Figure 2 | Autophagy is induced by *Candida* but does not play a role in *Candida* uptake by macrophages and neutrophils. (**a**) RAW-Blue cells (macrophage cell line) were cocultured with *Candida* labelled with Alexa Fluor-647 (AF-647; pink) for 0 or 60 min at the 1:1 ratio of Raw-Blue and spore cells. LC3 and nuclei were shown with green and blue, respectively. Corresponding Nomarski images are shown below. Scale bars = 5 μm. (**b**) Western blotting detection of LC3II in RAW-Blue cells stimulated with *C. albicans* (1:1 cell ratio) at the indicated time points. (**c**–**e**) BMDMs (**c**) and neutrophils (**d**) obtained from *Atg7* CKO and WT mice were fluorescently labelled and cocultured with AF-647-labelled *Candida* (1:5 ratio of host cells and *Candida* spores) for indicated duration. AF-647-positive cells were determined using flow cytometry. Intensity of AF-647 (*Candida*) in BMDMs at 30 min was assessed with flow cytometry analysis (**e**). The histogram is pre-gated on F4/80$^+$. (**f**) To determine macrophage reactive oxygen species production, dihydroethidium (DHE) staining in BMDMs was evaluated using flow cytometry 2 h after coculture with *Candida* (1:1 ratio of BMDMs and spores). (**g**–**i**) Inhibition of *Candida* expansion by BMDM (**g**,**h**) and neutrophils (**i**) was evaluated by the method described in the Methods section. *Candida* expansion with or without BMDMs was shown at indicated time points (**g**), and inhibition of *Candida* expansion was evaluated at 12 h after coculture with host cell culture. (**j**) Intensity of LC3 signals (green) in a *Candida* (pink)-engulfed RAW-Blue cell at 60 min after starting coculture was analysed along with the yellow line in the panel at right bottom. Scale bar = 2.5 μm. Shown in **a**,**j** are typical examples from 100 cells observed in four independent experiments. Results in **b**–**i** are representatives of at least two experiments with more than three mice per group. Error bars represent mean ± s.d. Student's *t*-test was used for statistical analysis. NS; not significant. $^{**}P<0.01$, $^{***}P<0.001$.

population in an uninfected condition (Fig. 3d,e). This suggests that *Atg7* CKO mice had less neutrophil egress from the BM than did WT mice. To further evaluate the neutrophil recruitment to infected sites, we injected *Candida* to the peritoneal cavity of *Atg7* CKO and WT mice. The lack of *Atg7* significantly reduced recruitment of neutrophils in the peritoneal cavity (Fig. 3f). Collectively, these results suggest the general and noteworthy contribution of autophagy in neutrophil recruitment to inflammatory sites.

We evaluated immune cells other than neutrophils in the spleen at 24 hpi. Proportions and numbers of splenic conventional DCs (cDCs) were slightly less in *Atg7* CKO mice than in WT mice (Supplementary Fig. 6b), suggesting that recruitment of cDCs was somewhat affected by autophagy. Proportions and numbers of plasmacytoid DCs (pDCs), B cells, CD8$^+$ and CD4$^+$ T cells did not show a significant difference between WT and *Atg7* CKO mice either before or after infection (Supplementary Fig. 6c). Numbers of F4/80^{lo} and F4/80^{hi} macrophage populations (gating strategy in Supplementary Fig. 6d), were also unaltered (Supplementary Fig. 6e). In sum, increased numbers of neutrophils recruited to inflammatory sites appear to be important in autophagy-mediated host resistance during the early stage of *Candida* infection.

Autophagy enhances production of neutrophil chemoattractants. CXCR2 deficiency in mice reduces neutrophil influx into *Candida*-infected sites and increases susceptibility to gastric

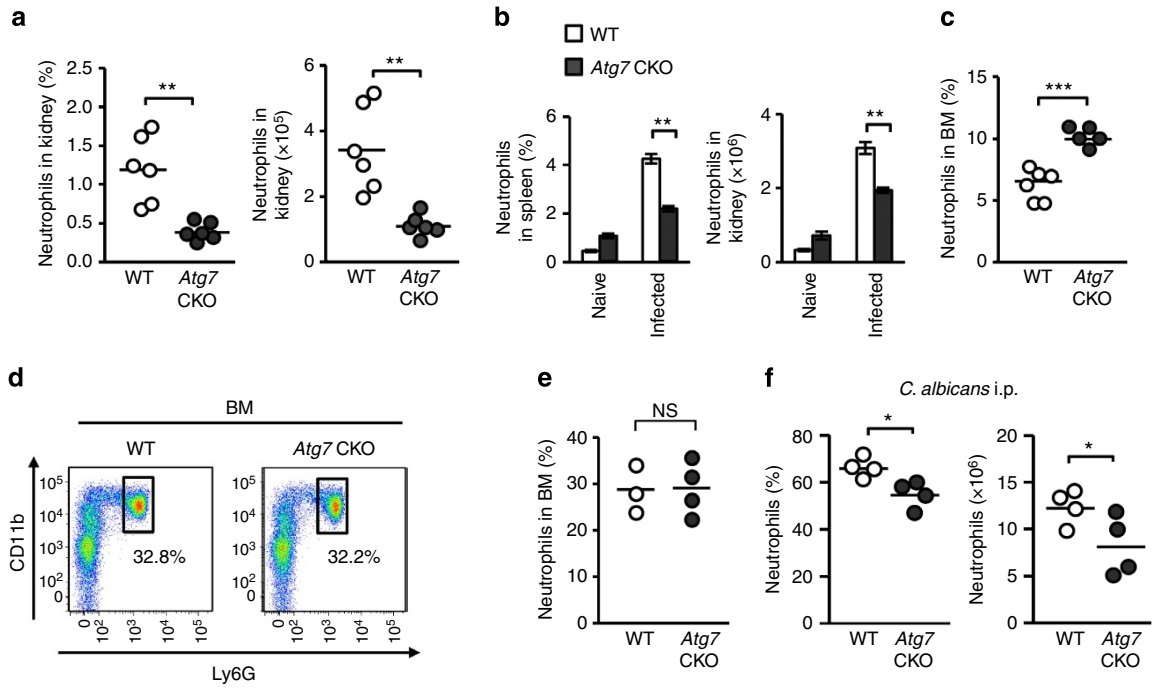

Figure 3 | Autophagy enhances neutrophil recruitment and clearance of *Candida*. Indicated mouse groups received *i.v.* injection of 10^6 *Candida* spores (except for **f**), and neutrophils ($CD11b^+Ly6G^+$) were enumerated in indicated organs 24 h post infection using flow cytometry. (**a**,**b**) Proportions and numbers of neutrophils in the kidney from WT and *Atg7* CKO mice (**a**); moreover, in the spleen from naive or infected WT mice (**b**, $n=4$). (**c**–**e**) Proportions of neutrophils in BM 24 h after *Candida* infection (**c**). Representative flow cytometry CD11b/Ly6G-staining patterns (**d**) and proportions (**e**) of neutrophils in BM in naive mice. WT and *Atg7* CKO mice were compared. (**f**) Proportions and numbers of neutrophils infiltrated into the peritoneal cavity at 18 h after *i.p.* injection of 5×10^6 *Candida* spores. One circle denotes a result from one mouse (**a**,**e**,**f**). Horizontal lines indicate the mean values. Data are representative of two independent experiments. Error bars represent mean ± s.d. Student's *t*-test was used for statistical analysis for **a**,**c**,**e**,**f**) and analysis of variance (ANOVA) was used for **b**. NS; not significant. $^*P<0.05$, $^{**}P<0.01$, $^{***}P<0.001$.

candidiasis and acute systemic candidiasis[32]. We first found that expression of CXCR2 was comparable between WT and *Atg7*-deficient neutrophils in the BM, peripheral blood and the spleen (Fig. 4a). Chemotactic ability towards CXCL1 and CXCL2, CXCR2 ligands, was also comparable between WT and *Atg7*-deficient neutrophils (Fig. 4b). These results suggested that *Atg7*-deficient neutrophils have normal migration ability. We next assessed levels of major neutrophil chemoattractants in the serum and kidney at 24 hpi. *Atg7* CKO mice showed significantly lower concentrations of both CXCL1 and/or CXCL2 in both the serum and kidney (Fig. 4c,d). These results suggest that autophagy increases neutrophil recruitment by enhancing production of chemoattractants at the site of inflammation, but not by enhancing the migratory ability of neutrophils.

Source of CXCL1 and CXCL2 early after *C. albicans* infection. To determine the cellular source of CXCL1 and CXCL2, we sorted splenic $F4/80^{hi}$ macrophages, $F4/80^{lo}$ macrophages, cDCs, pDCs, natural killer cells, T cells and B cells, by fluorescence-activated cell sorting (FACS) from spleens of WT mice at 24 hpi, and then cultured the cells for 24 h. $F4/80^{hi}$ macrophages were the only cell type that produced high levels of CXCL1 and CXCL2 (Fig. 5a). When $F4/80^{hi}$ macrophages were depleted from total splenocytes, the levels were significantly reduced (Fig. 5b). Thus, $F4/80^{hi}$ macrophages appear to be critical producers of CXCL1 and CXCL2.

Autophagy enhances chemokine production. We next examined the potential impact of *Atg7* deficiency in the production of CXCL1 and CXCL2 *in vivo*. At 24 hpi, splenic WT $F4/80^{hi}$ macrophages expressed significantly higher levels of *Cxcl1* and *Cxcl2* mRNA than did *Atg7*-deficient $F4/80^{hi}$ macrophages and $F4/80^{lo}$ macrophages of WT and $Atg7^{-/-}$ backgrounds (Fig. 6a). High levels of CXCL2 protein expression was also identified in splenic WT $F4/80^{hi}$ macrophages, but *not* in *Atg7*-deficient or $F4/80^{lo}$ macrophages in infected mice (Fig. 6b). Similarly, gene expression of *Ccl3* and *Ccl4* was highly expressed in splenic WT $F4/80^{hi}$ macrophages from infected mice (Supplementary Fig. 7a). (Note that CCL3 and CCL4 are ligands of C–C chemokine receptor 5, and act as chemoattractants for monocyte-derived macrophages and DCs[33].)

We have shown that ATG7-sufficient splenic $F4/80^{hi}$ macrophages produce high levels of chemokines both by *in vivo* and *ex vivo*. As *Candida* is accumulated in the kidney, we FACS-sorted renal $F4/80^{hi}$ macrophages and stimulated the cells with zymosan *ex vivo*. Again, the absence of ATG7 in the cells reduced CXCL2 production (Fig. 6c). We next tested chemokine expression in $F4/80^{hi}$ peritoneal macrophages, a dominant cell population in the peritoneal cavity of naive mice[21]. We obtained peritoneal-resident $F4/80^{hi}$ macrophages, and then stimulated the cells *ex vivo* with either zymosan (a cell wall component from *Saccharomyces cerevisiae*), heat-killed *C. albicans* (HKCA), Pam_3CSK_4 or curdlan. *Atg7*-deficient peritoneal $F4/80^{hi}$ macrophages again showed reduced expression of CXCL1, CXCL2, CCL3 and CCL4 at the level of mRNA and/or protein after cell stimulation, compared with WT cells (Fig. 6d,e; Supplementary Fig. 7b). As expected, WT peritoneal $F4/80^{hi}$ macrophages expressed significantly higher levels of chemokines compared with WT peritoneal $F4/80^{lo}$ (Supplementary Fig. 8a), as found in the splenic macrophages. The absence of ATG7 had no impact on CXCL2 production in $F4/80^{lo}$ peritoneal macrophages

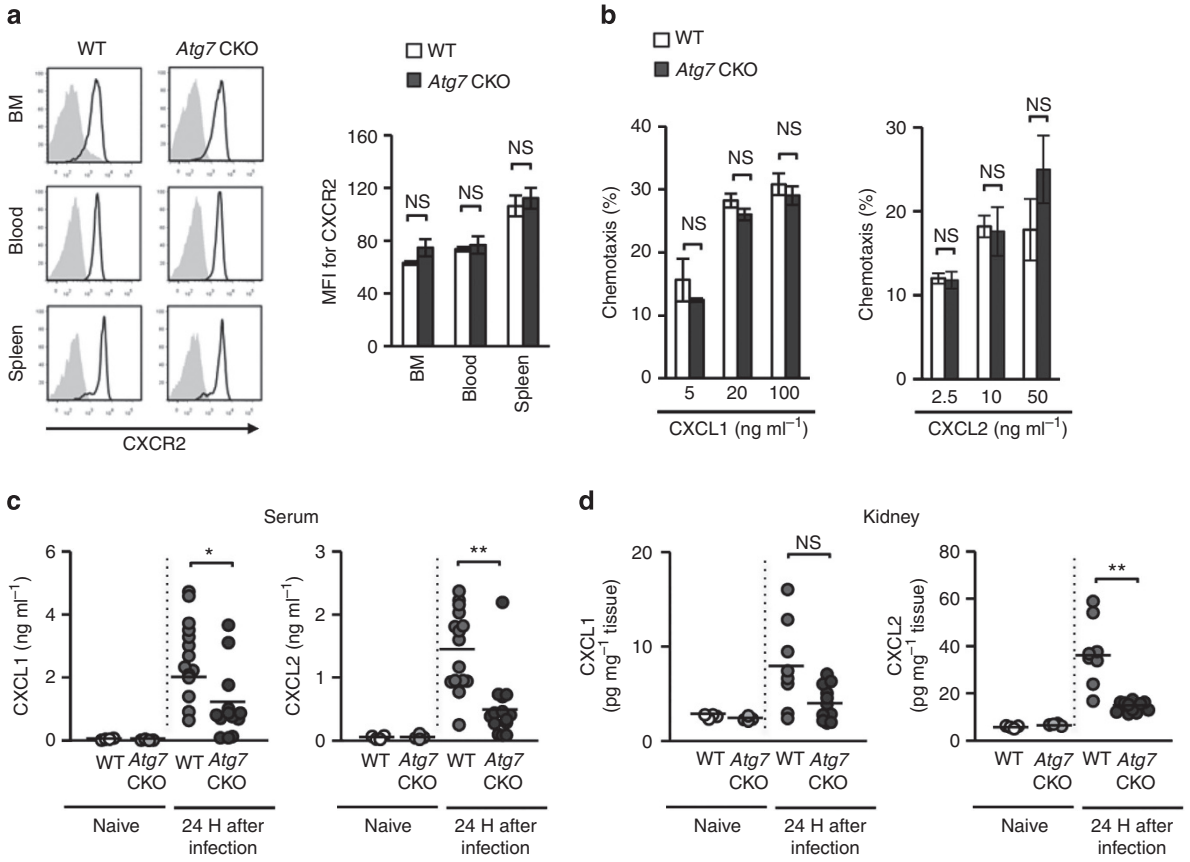

Figure 4 | Autophagy-induced levels of CXCL1 and CXCL2 in the serum and the kidney. (**a**) Histogram and mean fluorescent intensity (MFI) of CXCR2 staining determined with flow cytometry. Neutrophils were obtained from the BM, blood and spleen from WT and *Atg7* CKO mice at 24 h after *i.v.* injection of 10^6 *Candida* spores. (**b**) Transwell migration assay of neutrophils towards CXCL1 and CXCL2. Neutrophils were FACS-sorted as $CD11b^+Ly6G^+$ from the BM of naive mice and plated in the upper chamber of transwell. Indicated concentrations of CXCL1 and CXCL2 were added in the lower chamber. Cells were cultured for 1 h and the transmigration of neutrophils was assessed with flow cytometry. Data are representative of two independent experiments with at least three mice per each group (**a**,**b**). Error bars represent mean ± s.d. (**c**,**d**) Levels of chemokines in the serum (**c**) and the kidney (**d**) from WT and *Atg7* CKO mice. Naive and infected mice at 24 h after *i.v.* injection of 10^6 *Candida* spores were analysed. One circle denotes a result from one mouse. Horizontal lines indicate values of the mean. Error bars represent mean ± s.d. ANOVA was used for statistical analysis of **a**,**b** and Student's *t*-test was used for (**c**,**d**). NS, not significant. $^*P<0.05$, $^{**}P<0.01$.

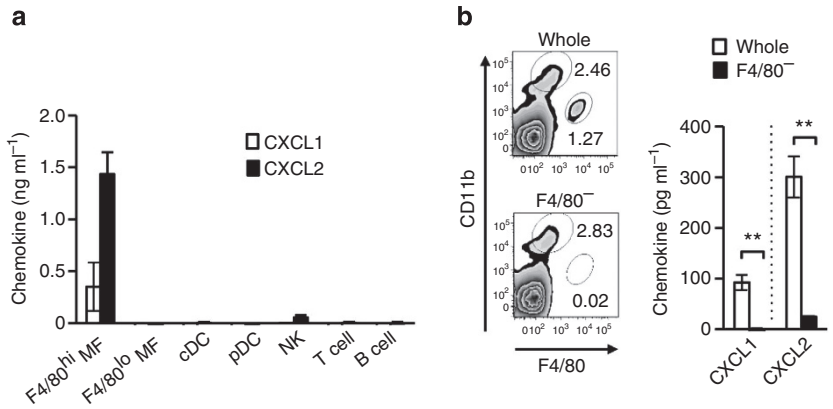

Figure 5 | F4/80^{hi} macrophages are a main source of CXCL1 and CXCL2 early after *Candida* infection. (**a**) CXCL1 and CXCL2 production by various splenic cell populations. Indicated splenic cell populations were purified using FACS from the spleen of mice 24 h after 10^6 *Candida i.v.* inoculation, and each population was cultured for 24 h (10^6 cells ml^{-1}). The chemokine production in the supernatants was assessed with enzyme-linked immunosorbent assay (ELISA). $n=3$. (**b**) Splenocytes were obtained from mice 24 h after *i.v.* injection of 10^6 *Candida* spores. F4/80^{hi} macrophage population was depleted by magnetic beads, and the rest of splenocytes were confirmed to be lacking the F4/80^{hi} population with flow cytometry (left panels). Whole splenocytes and F4/80^{hi} macrophage-removed splenocytes ($F4/80^-$) were cultured (5×10^7 ml^{-1}) for 24 h and chemokine production in the supernatants was evaluated with ELISA; $n=3$. Error bars represent mean ± s.d. Student's *t*-test was used for statistical analysis. $^{**}P<0.01$.

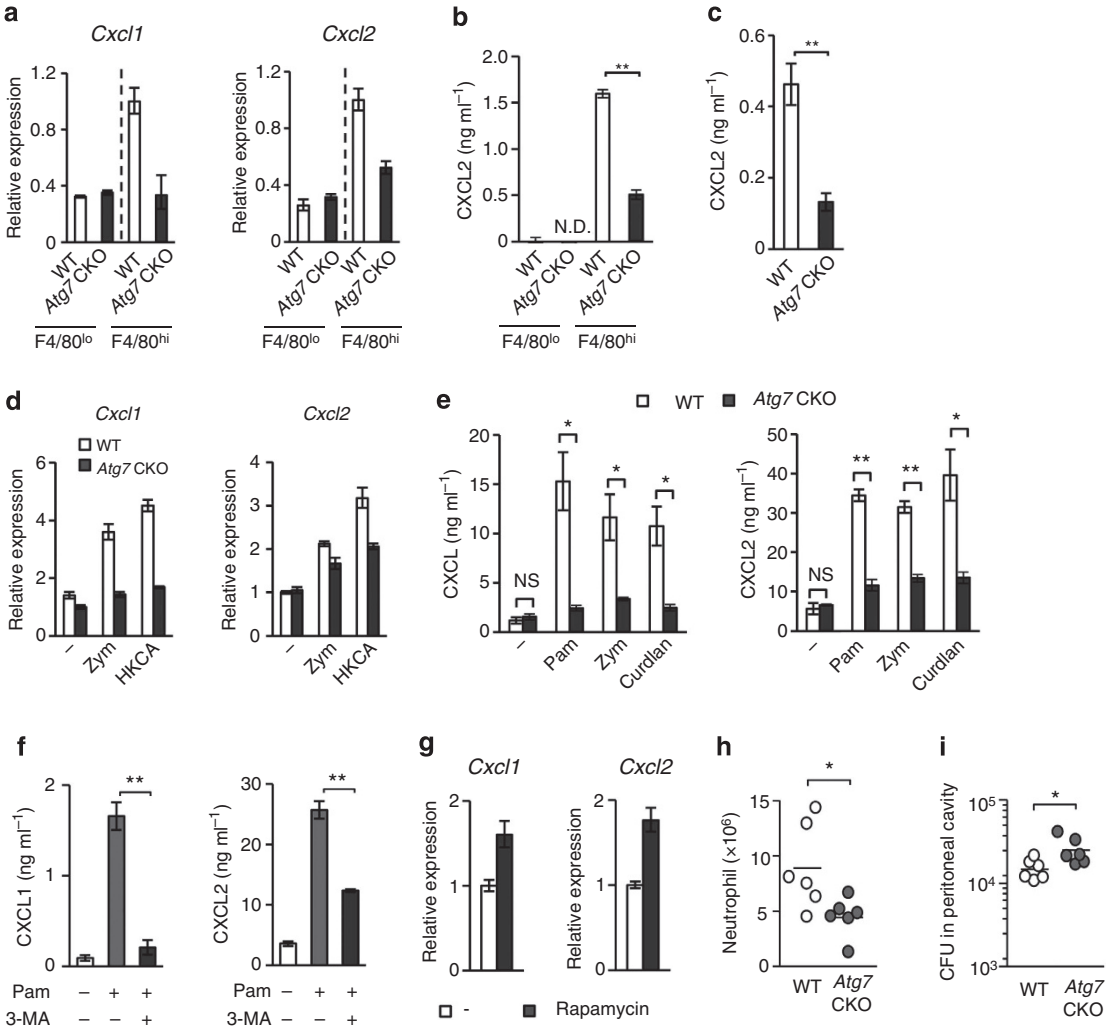

Figure 6 | ATG7 deficiency decreased chemokine production by F4/80^{hi} peritoneal-resident macrophages (**a**) Levels of *Cxcl1 and Cxcl2* mRNA in splenic F4/80^{lo} and F4/80^{hi} macrophages obtained from WT and *Atg7* CKO mice 24 hpi with 10^6 *Candida* spores. (**b**) Levels of CXCL2 protein in supernatants of macrophages subsets indicated in **a**. $n=3$. (**c**) CXCL2 levels in culture supernatants of renal F4/80^{hi} macrophages from naive mice. Cells were stimulated with zymosan (100 μg ml^{-1}) for 24 h. $n=3$. (**d**) Expression of *Cxcl1* and *Cxcl2* mRNA in peritoneal F4/80^{hi} macrophages obtained from naive mice. Cells were stimulated with zymosan (Zym; 100 μg ml^{-1}) or heat-killed *Candida* (HKCA; 5×10^5 ml^{-1}) for 3 h. (**e**) Levels of CXCL1 and CXCL2 proteins in culture supernatants of F4/80^{hi} peritoneal macrophages stimulated with Pam_3CSK_4 (Pam; 100 ng ml^{-1}), zymosan (100 μg ml^{-1}) or curdlan (100 μg ml^{-1}) for 24 h. $n=3$. (**f**) Peritoneal F4/80^{hi} macrophages were pretreated with 3-MA (10 mM), and then stimulated 2 h later with Pam_3CSK_4 (100 ng ml^{-1}) for additional 24 h. Supernatants were analysed with ELISA to measure CXCL1 (left panel) and CXCL2 (right panel) production. (**g**) Peritoneal F4/80^{hi} macrophages were pretreated with rapamycin (1 μg ml^{-1}) for 1 h, and then zymosan (100 μg ml^{-1}) was added and harvested 3 h later. *Cxcl1* and *Cxcl2* mRNA expression was assessed by real-time PCR analysis. $n=3$. (**h**,**i**) A million F4/80^{hi} peritoneal macrophages of WT or *Atg7* CKO F4/80^{hi} were transferred into the peritoneal cavity of *Atg7* CKO mice, and then 5×10^6 *Candida* spores were *i.p.* injected to the mice. Recruitment of neutrophils (**h**) and fungal burden (**i**) in the peritoneal cavity was evaluated 20 hpi. One circle denotes a result from one mouse. In all the experiments in Fig. 6, except for **h**,**i**, cells were pooled from at least three mice for one group to get enough numbers of macrophages. Data are representative of at least two independent experiments. Error bars for mRNA data denote RQ-Max/Min as described in the Methods section. Error bars for protein data represent mean ± s.d. ANOVA and Student's *t*-test were used for **e**,**f** and **b**,**c**, respectively. NS; not significantly different. *$P<0.05$ and **$P<0.01$.

(Supplementary Fig. 8b). Importantly, inhibition of autophagy with 3-methyladenine (3-MA) significantly reduced CXCL1 and CXCL2 production by WT F4/80^{hi} peritoneal macrophages stimulated with Pam_3CSK_4 (Fig. 6f). Indeed, induction of autophagy by rapamycin treatment *enhanced* the gene expression of *Cxcl1* and *Cxcl2* induced by zymosan (Fig. 6g). As an additional representative of F4/80^{lo} macrophages, BMDMs were also tested. *Atg7*-deficient BMDMs did not alter chemokine expression in CCL1, CCL2, CCL3 and CCL4 upon zymosan stimulation (Supplementary Fig. 9a). Further, treatment with rapamycin did not alter chemokine production by BMDMs (Supplementary Fig. 9b). Therefore, autophagy induces expression of tested chemokines in F4/80^{hi} macrophages but not in F4/80^{lo} macrophages.

We then tested whether mice, intraperitoneally transferred with *Atg7*-deficient F4/80^{hi} macrophages, have less ability to recruit neutrophils and clear *Candida*, compared with mice transferred with WT F4/80^{hi} macrophages. Less neutrophil recruitment and more fungal burden were identified in the peritoneal cavity of the recipients transferred with *Atg7*-deficient F4/80^{hi} macrophages compared with those with WT F4/80^{hi} macrophages (Fig. 6h,i), although *Atg7* deficiency in BMDMs

transferred to the peritoneal cavity of recipients did not affect neutrophil recruitment and *Candida* clearance (Supplementary Fig. 10). Taken together, results using various sources of macrophages suggested that ATG7 works through autophagy to induce chemokine production by F4/80^{hi} macrophages, and plays a critical role in neutrophil-mediated fungal clearance.

Autophagy does not affect cell death or receptor expression. We next sought to identify the mechanism for the autophagy-mediated induction of chemokine expression by F4/80^{hi} macrophages. First, there was no difference in cell survival between WT and *Atg7*-deficient F4/80^{hi} macrophages (Supplementary Fig. 11a). Inhibition of autophagy with 3-MA in RAW-Blue cells also did not alter the proportion of live cells, compared with untreated cells (Supplementary Fig. 11b). Absence of autophagy did not seem to affect the expression levels of PRRs (pattern-recognition receptors) that detect *Candida*, such as TLR2, TLR4, dectin-1 and dectin-2, in F4/80^{hi} macrophages from the spleen, kidney and peritoneal cavity following *Candida* infection (Supplementary Fig. 11c–e). While F4/80^{hi} macrophages produce higher levels of chemokines than do F4/80^{lo} macrophages, this phenomenon was also not explained by expression levels of TLR2, TLR4, dectin-1 and dectin-2 (Supplementary Fig. 12). These results suggested that autophagy contributes to enhancement of chemokine secretion in F4/80^{hi} macrophages without inhibiting cell death or upregulation of PRR expression.

Here we have evaluated the ability of host cells to phagocytose *Candida* and to inhibit *Candida* growth, as shown in Fig. 2 and Supplementary Figs 2 and 3, by using peritoneal F4/80^{hi} macrophages. Again, the absence of ATG7 in F4/80^{hi} macrophages did not alter *Candida* phagocytosis nor inhibited *Candida* growth, although LC3 puncta were clearly produced in WT F4/80^{hi} macrophages (Supplementary Fig. 13a–d). Interestingly, F4/80^{hi} macrophages were more susceptible than were F4/80^{lo} macrophages to intracellular germination of *Candida* (Supplementary Fig. 13e–g), suggesting that F4/80^{hi} macrophages are easily killed by *Candida* after completing their job as sentinels to recruit mainly neutrophils.

Autophagy enhances NFκB activation in F4/80^{hi} macrophages. A previous report showed that knockdown of either *Atg5* or *Atg7* inhibits NFκB signalling through TNFR[34]. Therefore, we sought to identify the mechanism in activation of NFκB, which induces gene expression of *Cxcl1*, *Cxcl2*, *Ccl3* and *Ccl4* (refs 35–37). We first confirmed that an NFκB inhibitor strongly suppressed CXCL1 and CXCL2 production by F4/80^{hi} peritoneal macrophages, stimulated with zymosan or HKCA (Fig. 7a). Indeed, *Atg7*-deficient F4/80^{hi} macrophages showed lower levels of NFκB activity than did WT F4/80^{hi} macrophages, as demonstrated by less IκB phosphorylation, greater IκB levels (that is, less IκB degradation; Fig. 7b), impaired NFκB p65 nuclear translocation (Fig. 7c; Supplementary Table 2) and impaired NFκB p65 binding to a target DNA promoter sequence (Fig. 7d). Inhibiting autophagy with 3-MA also downregulated NFκB activity in RAW-Blue cells detected with a secreted embryonic alkaline phosphatase (SEAP) reporter, and nuclear translocation assays (Supplementary Fig. 14a,b). Taken together, these results strongly suggest that autophagy positively regulates NFκB activation in F4/80^{hi} macrophages.

Autophagy sequesters A20 to induce NFκB activation. Since autophagy is known to specifically sequester certain proteins, we hypothesized that it also eliminates an NFκB signalling inhibitor to induce NFκB activity. For example, A20 is known to inhibit NFκB signalling[25,38] by deubiquitinating IκB kinase gamma (IKKγ; also known as NFκB essential modifier) and TRAF6 (ref. 39). A20-deficient mice spontaneously develop multiorgan inflammation and die prematurely[26]. Here we sought to show whether or not autophagy sequesters A20, particularly because A20 localize to an endocytic compartment upon stimulation with tumour necrosis factor (TNF)-α stimulation[40]. Stimulated *Atg7*-deficient peritoneal F4/80^{hi} macrophages indeed showed higher levels of A20 protein than did WT F4/80^{hi} macrophages (Fig. 8a; Supplementary Fig. 15). Our time course results of A20 levels showed a peak at 1 h after Pam_3CSK_4 stimulation for WT and *Atg7* CKO macrophages; however, the initial increase in *Atg7*-deficient F4/80^{hi} macrophages was much higher than that in WT cells (Fig. 8a,b). Even after the peak, *Atg7*-deficient F4/80^{hi} cells maintained A20 levels significantly higher than those of WT F4/80^{hi} cells (Fig. 8a,b). As expected from previous studies[26], the degree of NFκB activation showed a reverse correlation with A20 levels—weak NFκB activation in *Atg7* CKO macrophages than WT macrophages (Fig. 8a,b). Here we confirmed highly K63-deubiquitinated IKKγ, suggesting the increased impact of A20 in *Atg7* CKO F4/80^{hi} macrophages (Fig. 8c; negative controls in Supplementary Fig. 16a,b). ATG7-specific downregulation of A20 did not occur at the mRNA level (Fig. 8d), suggesting post-translational downregulation of A20 in WT F4/80^{hi} macrophages. Indeed, autophagy negatively regulated A20 protein levels as evidenced by 3-MA treatment on WT F4/80^{hi} macrophage increasing A20 expression 1 h after Pam_3CSK_4 stimulation (Fig. 8e).

Here we hypothesized that autophagy sequesters A20, and sought to first identify LC3 and A20 colocalization. (In this regard, we had to overexpress A20 in 3T3 cells, since detection of endogenous A20 by confocal microscopy was difficult.). Although A20 was not colocalized with LC3 in unstimulated cells (Supplementary Fig. 16c), their colocalization was identified after cell stimulation (Fig. 8f; Supplementary Table 3). To further evaluate the impact of autophagy-mediated A20 downregulation in CXCL1 expression, we used *Tnfaip3*$^{+/-}$ (A20 heterozygous knockout) peritoneal F4/80^{hi} macrophages, which have reduced levels of A20 expression compared with WT macrophages (Fig. 8g). (Knocking down A20 and using *Tnfaip3* homozygous knockout were not technically optional here, because of (1) poor *ex vivo* viability of F4/80^{hi} macrophages and (2) premature death in *Tnfaip3*$^{-/-}$ mice by multiorgan inflammation[25,26], respectively.) When autophagy was inhibited by 3-MA, CXCL1 production in WT cells was reduced, but no corresponding reduction was found in *Tnfaip3*$^{+/-}$ cells (Fig. 8h), suggesting that autophagic removal of abundant A20 in WT cells played a role in high CXCL1 production. Impact of inhibiting autophagy in *Tnfaip3*$^{+/-}$ macrophages was minimal due most likely to the fact that A20 was not sufficiently abundant in the *Tnfaip3*$^{+/-}$ cells to make a difference with or without autophagy (Fig. 8g). In summary, these results strongly suggest that NFκB is activated by autophagic sequestration of A20 in F4/80^{hi} macrophages.

p62 mediates the autophagic sequestration of A20. p62 is known as an adaptor protein that has a role in the selective delivery of target proteins to the autophagosome[41]. p62 was colocalized with A20 (Fig. 9a; Supplementary Fig. 16d; Supplementary Table 4) and co-immunoprecipitated with A20 (Fig. 9b; Supplementary Fig. 16e,f) in naive and stimulated cells. These results strongly suggest an interaction between p62 and A20. In addition, a deficiency of *Sqstm1,* encoding p62, increased protein levels of A20 in F4/80^{hi} macrophages (Fig. 9c; Supplementary Fig. 17a), in which chemokine production was subsequently reduced (Fig. 9d; Supplementary Fig. 17b). Collectively, it was thus suggested that p62 scavenges A20 to

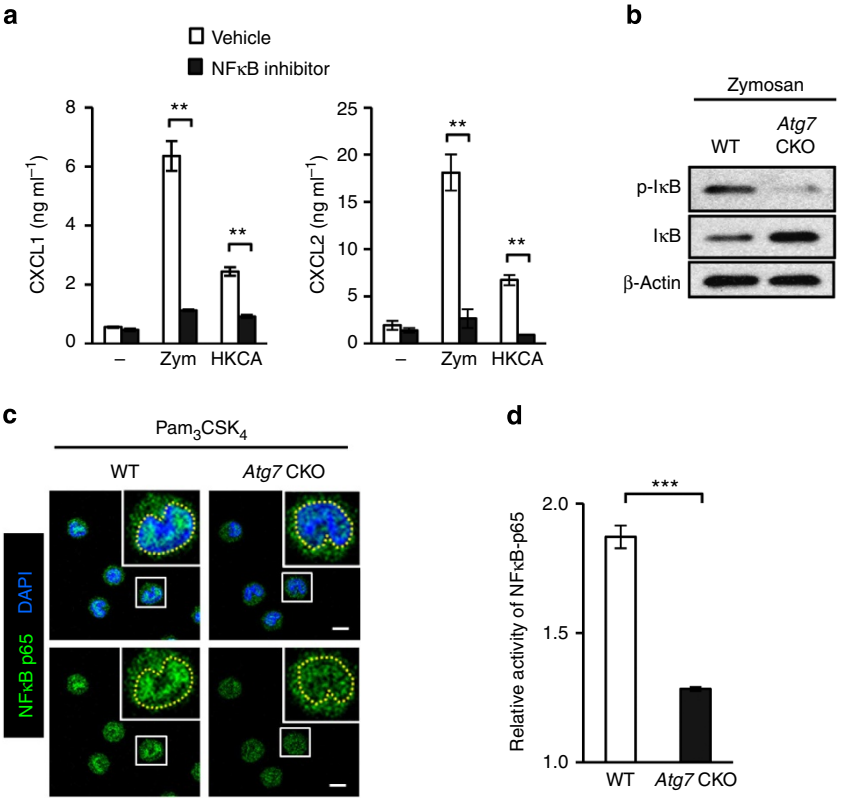

Figure 7 | Autophagy enhances NFκB activation in F4/80^{hi} macrophages. (**a**) Production of CXCL1 and CXCL2 by F4/80^{lo} and F4/80^{hi} peritoneal macrophages. Cells were stimulated with zymosan (100 μg ml^{-1}) or (HKCA; 5×10^5 spores per ml) for 24 h with or without an NFκB inhibitor, QNZ. Culture supernatants were analysed with ELISA. $n = 3$. (**b**) Western blot analysis of p-IκB and total IκB in F4/80^{hi} peritoneal macrophages stimulated with zymosan (100 μg ml^{-1}) for 30 min. (**c**) Translocation of NFκB p65 (green) to the nucleus (DAPI, blue) in F4/80^{hi} peritoneal macrophages stimulated with Pam_3CSK_4 (100 ng ml^{-1}) for 30 min. NFκB localization was analysed with confocal microscopy. Yellow broken lines in enlarged photos indicate borders of the nucleus. Shown are representative images from at least 50 cells. Scale bars indicate 5 μm. (**d**) Relative activity of NFκB in WT and *Atg7* CKO F4/80^{hi} peritoneal macrophages was evaluated. Cells were stimulated with zymosan (100 μg ml^{-1}) for 30 min, and p62 binding to a target NF-κB response element in DNA was evaluated with colorimetric reading. Values were calculated as a fold increase of OD values of stimulated cells from those of unstimulated cells. $n = 3$. Data are representative of two independent experiments. Error bars represent mean ± s.d. ANOVA and Student's *t*-test were used for statistical analysis of **a**,**d**, respectively. NS; not significant. ***$P < 0.001$.

autophagic degradation and that the downregulation of A20 enhances NFκB activity for chemokine production.

F4/80^{hi} macrophages express high levels of A20. We then asked why the autophagy-mediated NFκB activation is specific for F4/80^{hi} macrophages. F4/80^{hi} macrophages expressed higher levels of *Tnfaip3* (A20) mRNA than do F4/80^{lo} macrophages and BMDMs both with and without cell stimulation (Fig. 10a). Further, Western blotting showed high levels of A20 protein, particularly in *Atg7*-deficient F4/80^{hi} macrophages after zymosan stimulation, while levels of A20 in F4/80^{lo} macrophages were too weak to be detected regardless of *Atg7* deficiency (Fig. 10b). Even without stimulation, F4/80^{hi} macrophages expressed A20 protein abundant enough to be detected in by western blotting (Supplementary Fig. 16e,f). These results suggest that F4/80^{hi} macrophages express higher levels of A20 than do F4/80^{lo} macrophages regardless of cell stimulation. In addition, A20 and p62 appeared to constitutively interact (Supplementary Fig. 16e), suggesting that A20 is ready to be sequestered in autophagsomes with p62 as soon as autophagosomes appear. Sequestration of A20 in F4/80^{hi} macrophages by autophagy thus appears to be a critical event for robust NFκB activation upon fungal infection. Deficiency of autophagy allows accumulation of A20 in F4/80^{hi} macrophages, presumably contributing to the defect in their chemokine expression. Our results here suggest that tissue-resident F4/80^{hi} macrophages take advantage of autophagy to sequester intrinsically abundant A20 for the activation of NFκB in an effort to quickly respond to fungal infection (Fig. 10c).

Discussion

In viral, bacterial and parasitic infections, autophagy contributes to host protection by containing pathogens in the autophagosome for pathogen clearance[1–3]. Autophagy also promotes phagocytosis and antigen processing in these microbial infections[42–44]. On the basis of these findings, we initially expected the involvement of autophagy in the direct killing of fungal pathogens. However, the data in this study demonstrated that ATG7 did not affect *Candida* phagocytosis or the inhibition of *Candida* expansion by macrophages and neutrophils. Unexpectedly, our intensive search did not identify LC3 cargos containing live *Candida* spores, although zymosan particles successfully recruited LC3. In line with our findings, an *in vivo* study using zebrafish also demonstrated that very few conidia of *C. albicans* were contained in LC3 cargos[45]. In addition, a recent study showed that live *Candida* did not induce clear LC3 staining surrounding conidia, while HKCA and β-1,3-glucan-coated polystyrene beads were clearly engulfed by LC cargos[46], suggesting that live *Candida* somehow escapes from uptake by LC3 cargos. Although the possibility of transient inclusion of live *Candida* in LC3 cargos has not been ruled out, host cells do not

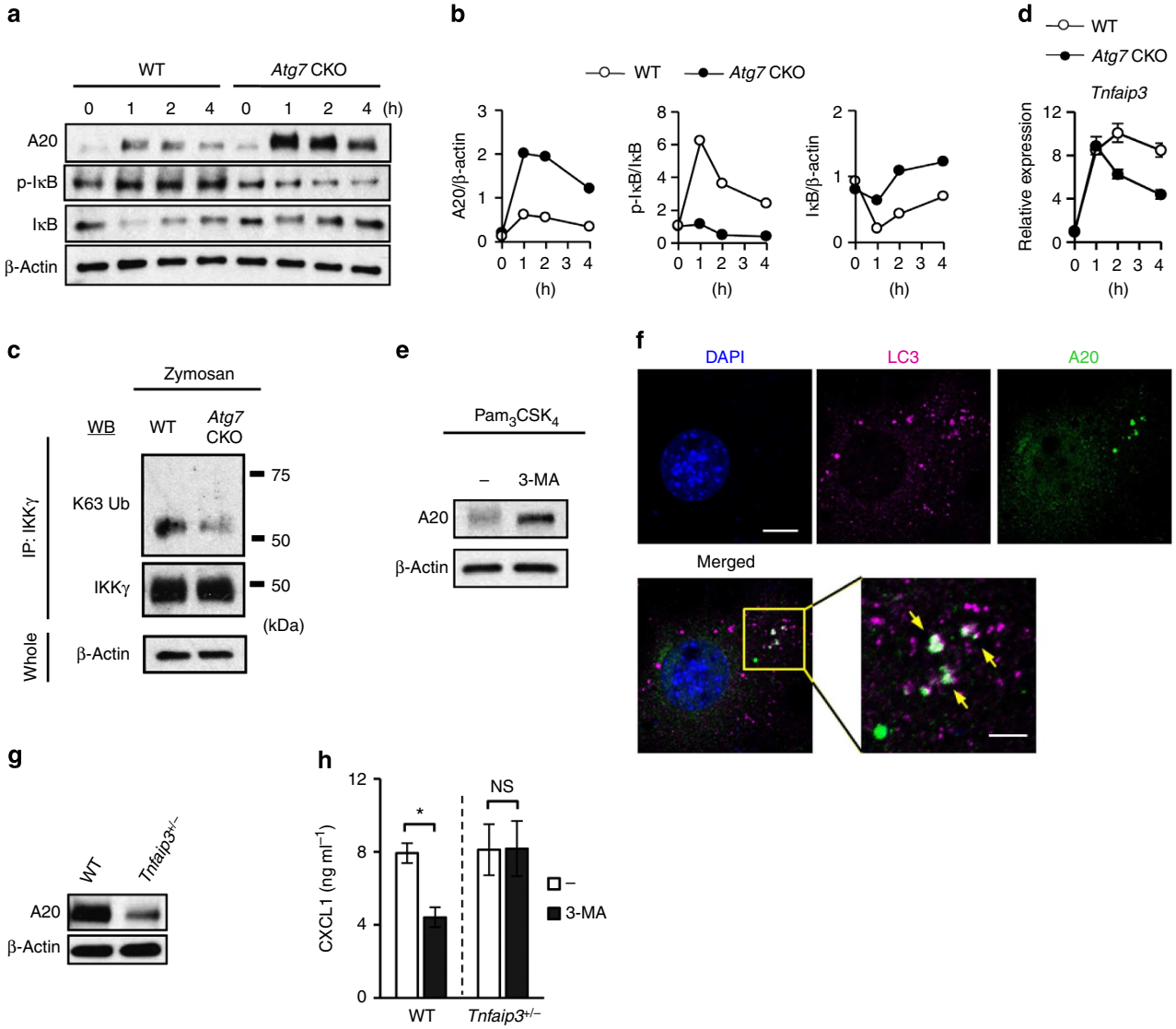

Figure 8 | Absence of ATG7 decreases A20 levels in F4/80^{hi} macrophages. (**a**,**b**) Turnover of A20, p-IκB and total IκB protein levels in F4/80^{hi} peritoneal macrophages (WT versus *Atg7* CKO) stimulated with Pam_3CSK_4 (100 ng ml^{-1}). Cell lysates were harvested at indicated time points and submitted for western blot detection (**a**). Abundance of proteins evaluated by densitometry was plotted for A20, p-IκB normalized, total IκB normalized with β-actin, total IκB and β-actin, respectively. (**c**) Detection of K63-ubiquitination of IKKγ. F4/80^{hi} peritoneal macrophages were stimulated with zymosan (100 μg ml^{-1}) for 30 min. IKKγ was immunoprecipitated and K63-ubiquitination of IKKγ was detected by immunoblotting with K63-Ub antibody. Results of negative control using unstimulated cells and control IgG are shown in Supplementary Fig. 15a,b. (**d**) Expression of *Tnfaip3* mRNA in F4/80^{hi} peritoneal macrophages (WT versus *Atg7* CKO) stimulated with Pam_3CSK_4 (100 ng ml^{-1}) for indicated duration. Evaluated by qPCR. Error bars for mRNA data denote RQ-Max/Min as described in the Methods section. (**e**) Expression of A20 in peritoneal F4/80^{hi} macrophages stimulated by Pam_3CSK_4 (100 ng ml^{-1}) for 1 h in the absence or presence of 3-MA (5 μM). (**f**) Confocal microscopy analysis to localize A20 and LC3. NIH-3T3 cells were transfected with V5-tagged A20 expression vector, and stimulated with Pam_3CSK_4 (100 ng ml^{-1}) for 60 min. LC3 and V5 antibodies were used to detect LC3 and A20, respectively. Scale bars in unmagnified and magnified panels indicate 10 and 4 μm, respectively. A20, LC3, and nuclei were shown with green, pink and blue, respectively. White arrows indicate colocalization of A20 and LC3. (**g**) Western blot detection of A20 in naive peritoneal F4/80^{hi} macrophages obtained from WT and *Tnfaip3*$^{+/-}$ mice. (**h**) Levels of CXCL1 in culture supernatants of WT and *Tnfaip3*$^{+/-}$ F4/80^{hi} macrophages stimulated with Pam_3CSK_4 (100 ng ml^{-1}) for 24 h. Indicated groups were treated with 3-MA (3 μM) starting an hour before the addition of Pam_3CSK_4. CXCL1 production was evaluated with ELISA. $n=3$. Data shown in all the panels are representatives of at least two independent experiments. Error bars represent mean ± s.d. Student's *t*-test was used. NS; not significant. $^*P<0.05$.

appear to directly kill *Candida* in autophagosomes and LC3-associated phagosomes.

A recent article reported that disruption of host autophagy *ex vivo* by *Atg5* shRNA in a macrophage cell line decreased the phagocytic index of *Candida*, as well as the level of *Candida*-killing activity[8]. This result is not quite the same as what we found here; however, multiple differences exist between the earlier study's experimental conditions and ours, as follows: the study[8] used the SC5314 *Candida* strain, *Atg5* knockdown in J774.16 cell lines, and evaluated phagocytosis and *Candida*-killing activity at 30 min. On the other hand, we used *Atg7* CKO in BMDMs, splenic macrophages, thioglycollate-elicited peritoneal macrophages and neutrophils (Fig. 2c–e; Supplementary Figs 2 and 3). We also evaluated phagocytosis at 0.5, 1, 2 and 3 h, as well as the inhibition of *Candida* expansion at 1.5, 3, 6 and 12 h. Despite these differences, a key conclusion of our study is the

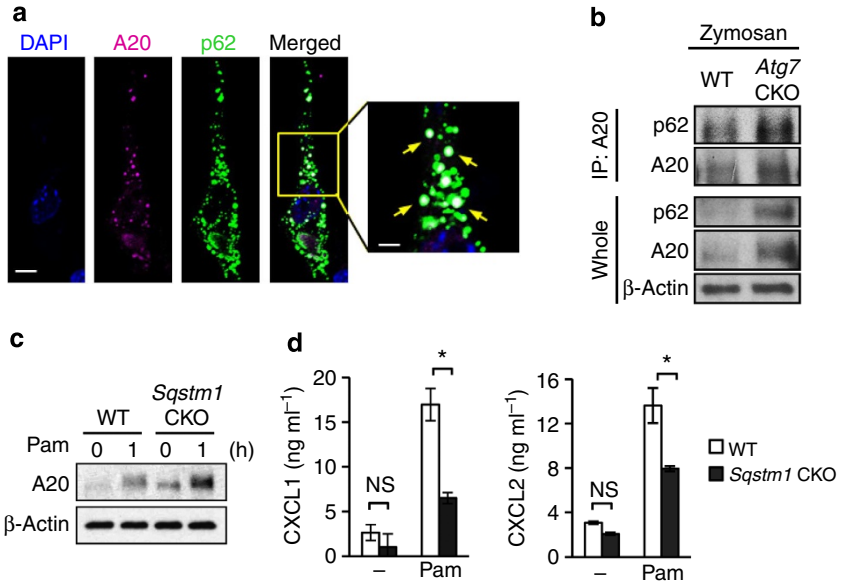

Figure 9 | p62 mediates A20 sequestration by autophagy. (**a**) Colocalization of A20 and p62 was evaluated with confocal microscopy. NIH-3T3 cells expressing exogenous A20-V5 and p62-HA were stimulated with Pam_3CSK_4 (100 ng ml^{-1}) for 60 min, and A20 (pink) and p62 (green) were detected by V5 and HA antibodies, respectively. Yellow arrows indicate co-localization of A20 and p62. Scale bar = 10 μm. (**b**) Co-immunoprecipitation of A20 and p62. Peritoneal F4/80^{hi} macrophages were stimulated with Pam_3CSK_4 (100 ng ml^{-1}) for 60 min. Cell lysates were immunoprecipitated with A20 antibody, and then p62 was detected with p62 antibody by western blotting. Results for negative controls using unstimulated cells and control IgG are shown in Supplementary Fig. 15e,f. (**c**) Expression of A20 in WT and p62 (*Sqstm1*)-deficient peritoneal F4/80^{hi} macrophages, which were unstimulated or stimulated with Pam_3CSK_4 (100 ng ml^{-1}) for 1 h. (**d**) CXCL1 and CXCL2 production by WT and p62 (*Sqstm1*)-deficient peritoneal F4/80^{hi} macrophages. Macrophages were stimulated with Pam_3CSK_4 (100 ng ml^{-1}) for 24 h, and chemokine levels in the culture supernatants were evaluated by ELISA. $n = 3$. Data in all the panels are representative of at least two independent experiments. Error bars represent mean ± s.d. ANOVA was used for statistical analysis. NS; not significant. *$P < 0.05$.

same as the previous report[8] in terms of the involvement of autophagy in host protection against *Candida*. We should also note another recent research effort that found only slightly worse survival from *Candida* infection in *Atg7* CKO (LysM-Cre) mice[9]. One possible explanation of the latter is that the recent study[9] used another different *Candida* strain, because *Candida* strains are indeed known to have a significant impact on host responses[47,48].

Here we demonstrated autophagy-mediated induction of chemokine expression by sequestering an NFκB inhibitor, A20, in a manner specific to the F4/80^{hi} macrophage population at the least in spleens, the peritoneal cavity and the kidney during systemic *Candida* infection. A20 is also known to act as a negative regulator of autophagy[49], suggesting that fine-tuning of inflammatory responses by feedback between A20 and autophagy is also possible in F4/80^{hi} tissue-resident macrophages. A20 works in TLR and TNFR signalling pathways, and protects hosts from collateral damage due to excessive inflammation initiated by viral and bacterial infections[25–27,50]. However, the role of A20 in fungal infection has not yet been reported. Here we suggest that abundant A20 in F4/80^{hi} macrophages is an obstacle to jump-start early innate immune responses in fungal infections. Thus, F4/80^{hi} macrophages are able to take advantage of autophagy and remove A20, since the cell type already has high levels of A20. The removal of A20 by autophagy in F4/80^{hi} macrophages subsequent to infection is thus an effective approach to address infection, and prepare for the next step, that is, recruitment of neutrophils. Given that *Atg7* CKO mice are susceptible to *Candida* infection at an early stage, autophagy in F4/80^{hi} macrophages appears to be a critical and effective intervention, particularly at these earlier stages.

A previous report demonstrated that autophagy eliminates BCL10, and inhibits NFκB activity in T cells upon T-cell receptor stimulation[5]. On the other hand, our results clearly indicate that autophagy enhances NFκB signalling by eliminating A20 in F4/80^{hi} macrophages. Since BCL10 is also expressed in macrophages, it is possible that BCL10 is also sequestered by autophagy in macrophages upon PRR stimulation; however, the autophagy-mediated depletion of BCL10 in macrophages may not have the impact it does in T cells, because signalling pathways inhibited by A20 have a significant impact on responses of macrophages. It is therefore likely that outcomes of autophagy are not the same between different cell types because of their distinct signal transduction networks.

We have shown that autophagy removes abundant A20 in F4/80^{hi} macrophages for copious production of CXCL1/2. Here F4/80^{lo} macrophages also perform autophagy and do not express abundant A20 as F4/80^{hi} macrophages do. Nevertheless, F4/80^{lo} macrophages express low levels of CXCL1/2. Although further investigation is necessary to better explain why F4/80^{lo} macrophages do not produce CXCL1/2 as well as F4/80^{hi} macrophages, mechanistic machineries to produce the chemokines between the subsets appear to differ. For example, it is possible that expression of *Cxcl1* and *Cxcl2* genes in F4/80^{lo} macrophages may require a higher threshold of PRR signalling intensity than that in F4/80^{hi} macrophages. A possible impact of negative regulators on chemokine expression, other than A20 in F4/80^{lo} macrophages, cannot be ruled out as well. At the least, the ability to express high levels of CXCL1/2 by F4/80^{hi} macrophages as tissue-resident sentinels in the kidney, spleen and peritoneum is biologically relevant for early antifungal immunity; moreover, F4/80^{hi} macrophages may have further developed a mechanism for quickly secreting high levels of chemokines during the course of evolution.

Hosts are protected from hyperinflammation and autoimmunity by the inhibitory effect of A20. At the same time, A20

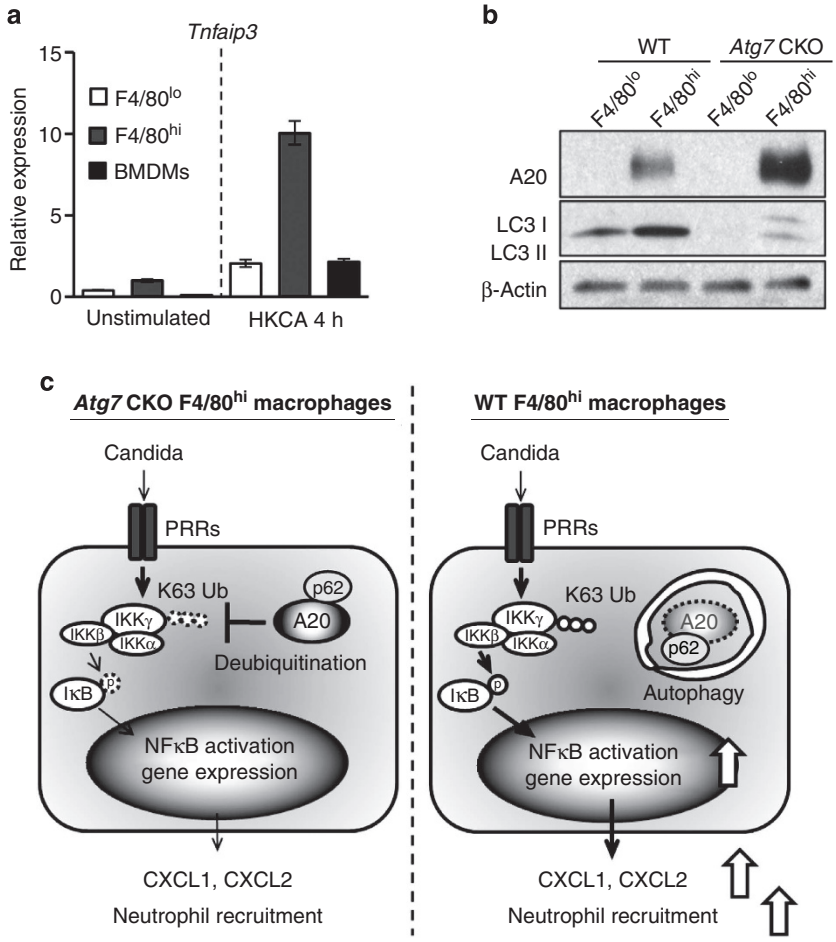

Figure 10 | A20 is highly expressed in F4/80^{hi} peritoneal macrophages, but not in F4/80^{lo} peritoneal macrophages. (**a**) Comparison of *Tnfaip3* mRNA levels among F4/80^{lo} and F4/80^{hi} peritoneal macrophages and BMDMs. Unstimulated and stimulated cells with HKCA (5×10^5 ml^{-1}, 1:1 ratio) for 4 h were analysed with real-time PCR. Error bars denote RQ-Max/Min as described in the Methods section. (**b**) Western blot analysis of A20 and LC3 expression in F4/80^{lo} and F4/80^{hi} peritoneal macrophages stimulated with zymosan (100 μg ml^{-1}) for 30 min. Data are representative of two independent experiments (**a**,**b**). (**c**) Schematic illustration of autophagy-mediated NFκB activation in F4/80^{hi} macrophages and the resulting induction of resistance to *Candida* infection. F4/80^{hi} macrophages induce autophagy upon *Candida* detection. Autophagy then sequesters abundant A20 through interaction between p62 and A20, and then unleashes NFκB activity in F4/80^{hi} macrophages. As a result, the macrophages secrete high levels of CXCL1 and CXCL2 to recruit neutrophils for fungal clearance.

becomes an obstruction when activation of immune responses is necessary during infections. For exerting rapid and strong immune responses, autophagy quickly sequesters inhibitory molecule A20, which is bound by p62 even before cell stimulation, in F4/80^{hi} macrophages for them to enhance NFκB activation for producing neutrophil chemoattractant (Fig. 10c). Autophagy plays a crucial role in early antifungal immunity by jump-starting the innate immune system in F4/80^{hi} macrophages, which are largely tissue-resident macrophages[18–21]. It would be helpful if future research efforts focus on whether or not targeted manipulation limited to tissue-resident macrophages is possible. This would allow researchers to further dissect the biology of tissue-resident macrophages *in vivo*. Results from the current study suggest that F4/80^{hi} macrophages do, indeed, play the role of a sentinel of immunity at the front lines of infection by utilizing autophagy.

Methods

Mice and cell preparation. All the mice used here are on the C57BL/6 background. *Atg7*$^{fl/fl}$, *Tnfaip3*$^{-/-}$ and *Sqstm1*$^{fl/fl}$ mice were described previously[51–53]. *LysM*$^{cre/cre}$ mice were purchased from Jackson Laboratories. Six- to eight-week-old sex-matched WT, *Atg7* CKO, *Tnfaip3*$^{+/-}$ or *Sqstm1*CKO mice were used for all experiments. All the experiments were performed as approved by the Institutional Animal Care and Use Committee. Complete RPMI medium (10% (vol/vol) fetal bovine serum, penicillin/streptomycin (Sigma), 2 mM of L-glutamine; Life technologies)) was used for host cell culture. RAW-Blue cells were purchased from Invivogen. F4/80^{hi} and F4/80^{lo} macrophages were isolated from the kidney or peritoneal cavity using FACS isolation as CD11b$^+$Ly6G$^-$F4/80^{hi} and CD11b$^+$Ly6G$^-$F4/80^{lo}, respectively. Splenic F4/80^{hi} and F4/80^{lo} macrophages were isolated as AF$^+$Ly6G$^-$F4/80^{hi} and CD11b$^+$Ly6G$^-$F4/80^{lo} after gating out SSC^{hi} (eosinophils). BMDMs were derived by culturing BM cells with L929 conditioned medium (15%, vol/vol) for 7 days as previously described[54]. Thioglycollate-elicited macrophages and neutrophils were obtained from the peritoneal cavity 3 days and 1 day, respectively, after intraperitoneal (*i.p.*) injection of thioglycollate (3%, 2.5 ml per mouse). For some experiments, thioglycollate-elicited macrophages and neutrophils were purified by MACS beads (Myltenyi) as CD11b$^+$ and Ly6G$^+$ cells, respectively. Total splenic CD11b$^+$ macrophages were purified from the spleen of naive mice with CD11c-MACS beads (Myltenyi). For chemotaxis assay, neutrophils were FACS-purified from BM of naive mice as CD11b$^+$Ly6G$^+$. On the other hand, thioglycollate-elicited peritoneal neutrophils were used for phagocytosis and *Candida* inhibition assay. In some experiments, macrophages were stimulated with Pam_3CSK_4 (100 ng ml^{-1}), Curdlan (100 μg ml^{-1}), zymosan (100 μg ml^{-1}) or heat-killed *C. albicans* (HKCA; 5×10^6 ml^{-1}).

Antibodies, reagents and major machines for analyses. Antibodies against CD11b (clone: M1/70), F4/80 (BM8), TLR4 (MTS510), TLR2 (T2.5), CXCR2 (TG11), CD4 (GK1.5), CD3 (17A2), CD11c (N418) and β-actin were purchased from BioLegend and used at a 1/200 dilution. Antibodies against CD8 (53–6.7),

Ly6G (1A8) and B220 (RA3-6B2) were from BD Bioscience (1/200 dilution). Dectin-1 (2A11) and dectin-2 (D2.11E4) antibodies were from AbD Serotec (1/100 dilution). IκB (L35A5), phosphorylated IκB (14D4), p62 (5114S), K63-ubiquitin (5621S) and LC3A/B (4108S; 1/1,000 dilution for western blotting) antibodies were purchased from Cell Signaling Technology. LC3 (ab51520; 1/200 dilution for immunofluorescence), IKKγ (ab7890; 1/1,000 dilution for western blotting) antibodies were purchased from Abcam. Antibody against His (HIS.H8; 1/200 dilution) was purchased from Thermo Scientific. V5 antibody (PAB11383; 1/5,000 dilution) and HA antibody (HA-7; 1/1,000 dilution) were purchased from Abnova and Sigma, respectively. A20 monoclonal antibody (A-12; 1/50 dilution for immunoprecipitation and western blotting) and IKKγ antibody (FL-419; 2 μg for 200 μg proteins, for immunoprecipitation), NFκB p65 polyclonal antibody (sc-109; 1/50 dilution), 3-MA, rapamycin and NFκB inhibitor (QNZ) were purchased from Santa Cruz. Recombinant CXCL1 was purchased from BioLegend. Pam_3CSK_4 and curdlan were purchased from Invivogen. Zymosan was purchased from MP Biomedicals. FACS-sorting with MoFlo Legacy (Beckman Coulter) was used for some experiments. Sorted cell populations we used were confirmed to be >95% of purity. FACS Canto II (BD) was used for flow cytometry. Mastercycler realplex^2 and Mastercycler proS (Eppendorf) were used for real-time PCR and conventional PCR, respectively. Zeiss 710 confocal microscopy and the Zeiss Efficient Navigation (ZEN; Carl Zeiss) softwares were used for data acquisition and analysis, respectively. The Fiji software (http://fiji.sc/Fiji) was used to determine the intensity of fluorescence.

***Candida* infection, evaluating fungal burdens and histology.** Sex-matched mice of age 6–8 weeks were infected by intravenous (*i.v.*) injection of *C. albicans* (ATCC 18804). In some experiments, the same strain of *Candida* (5×10^6 spores per mouse) was intraperitoneally injected. Body weights and survival of mice were evaluated every 24 h until whichever comes first either 18 days post infection or reaching at the human end point approved by the mouse protocol. To measure *in vivo* fungal burdens, tissue lysates from kidneys and spleens (or fluids from peritoneal lavage) were first treated with H_2O to lyse host cells (but *C. albicans* is not lysed by water), and then plated on YPD agar plates and incubated overnight to determine *Candida* colony-forming units (CFUs). For histological analysis, tissues were harvested 3 days after *Candida* infection (10^6 *i.v.*) and submitted for haematoxylin and eosine and silver staining.

Evaluating *Candida* uptake and intracellular germination. Macrophages and neutrophils were stained with antibodies against CD11b, F4/80 (for macrophages) or Ly6G (for neutrophils), and cocultured with same number of Alexa Fluor 647 (AF647)-labelled *C. albicans* (host cell versus *Candida* spore numbers as the 1:1 ratio). Cells were fixed with 2% (wt/vol) paraformaldehyde and submitted for flow cytometry. Proportions of AF647-positive host cells were evaluated for macrophages ($CD11b^+F4/80^+$) and neutrophils ($CD11b^+Ly6G^+$). Since this method also picks up host cells simply attaching to *Candida* without phagocytosis, we also evaluated cells by confocal microscopy and eye-counted the cells that completely engulfed *Candida*. As expected, percentages of AF647-positive cells were larger than those of *Candida*-engulfed cells evaluated by eye-counting; however, the differences in the percentages were proportional and flow cytometry analysis could be used as a substitute to evaluate phagocytosis between groups used in this study. To evaluate *Candida* germination, coculture of *Candida* and host cells were set up as described above for the uptake analysis, except that cells were cultured and fixed directly on cover glasses for confocal microscopic analysis. To evaluate host cell death, the live/dead Fixable Violet Dead Cell Stain Kit (Life technologies) was used and dead cells were enumerated with flow cytometry.

Evaluating inhibition of *Candida* expansion. Macrophages (BMDMs, thioglycollate-elicited macrophages, splenic $CD11b^+$ macrophages and peritoneal $F4/80^{hi}$ macrophages) and thioglycollate-elicited neutrophils were used for the analyses. To evaluate host cells to inhibit *Candida* expansion, live *Candida* was cocultured with host cells at the 1:10 (conidia:host) ratio (termed 'test samples'). Negative control culture had *Candida* alone. Twelve hours after coculture, host cells were lysed with water and *Candida* CFU was determined with YPD plates. Results were obtained with the following formula: *Candida* Expansion (fold) = [CFU at 12 h]/[CFU at 0 h]; inhibition of *Candida* expansion (%) = (1 − [CFU of test samples at 12 h]/[CFU of negative control at 12 h]) × 100.

Evaluation of NFκB activity. NFκB activity was evaluated by either one or combination of the following methods. First RAW-Blue cell line (Invivogen), harbouring an NFκB reporter to express SEAP, was used with QUANTI-Blue (Invivogen) to detect SEAP activity with a plate reader (TECAN), as indicated by the manufacturer. RAW-Blue cells express PRRs, such as TLRs and dectin-1. Second, functional NFκB activity was carried out by evaluating the binding of p65 to a target DNA fragment with the NFκB p65 Transcription Factor Assay kit (Thermo scientific). Third, nuclear translocation of NFκB p65 was evaluated by confocal microscopy. Fourth, biochemical analyses to detect phosphorylation of IκB and reduction of total IκB were also carried out by immunoblotting detection.

Neutrophil chemotaxis assay. Neutrophils were FACS-sorted from the BM of naive mice as $CD11b^+Ly6G^+$. Neutrophils (5×10^5) were plated in the upper chamber of transwell (3-μm pore size; Corning), and CXCL1 was added in the lower chamber. After 1 h of incubation at 37 °C, numbers of migrated cells were determined. Proportion of migrated cells was calculated as follows: chemotaxis (%) = {[cell number in the lower chamber with CXCL1] − [cell number in the lower chamber without CXCL1]/(5×10^5)} × 100.

Quantitative PCR analysis. mRNA expression levels were determined with real-time PCR using the $\Delta\Delta C_t$ method with the KAPA SYBR fast qPCR Master Mix (KAPA Biosystems) and the following primer sets: *Cxcl1* (forward: 5′-TGGGATTCACCTCAAGAACA-3′, reverse: 5′-TTTCTGAACCAAGGGAGCTT-3′), *Cxcl2* (forward: 5′-CCACCAACCACCAGGCTAC-3′, reverse: 5′-GCTTCAGGGTCAAGGGCAAA-3′), *Ccl3* (forward: 5′-ACTGCCTGCTGCTTCTCCTACA-3′, reverse: 5′-AGGAAAATGACACCTGGCTGG-3′), *Ccl4* (forward: 5′-AAACCTAACCCCGAGCAACA-3′, reverse: 5′-CCATTGGTGCTGAGAACCCT-3′), *Tnfaip3* (forward: 5′-TTTGCTACGACACTCGGAAC-3′, reverse: 5′-TTCTGAGGATGTTGCTGAGG-3′), *Atg7* (forward: CAGGACAGAGACCATCAGCTCCAC, reverse: TGGCTGCTACTTCTGCAATGATGT) and *Actb* (forward: 5′-TGTTACCAACTGGGACGACA-3′, reverse: 5′-CTGGGTCATCTTTTCACGGT-3′). *Actb* expression was used as an internal control. Results shown are representatives from multiple independent experiments with similar results. Error bars calculated were based on the calculation of RQ-Min = $2^{-(\Delta\Delta Ct + T \times s.d.(\Delta Ct))}$ and RQ-Max = $2^{-(\Delta\Delta Ct - T \times s.d.(\Delta Ct))}$ from triplicate wells as suggested by a manufacturer of PCR machines (Applied Biosystems). $T \times s.d.(\Delta Ct)$ is a square root of x^2+y^2, where x and y are standard deviations of Ct values for a gene of interest and an internal control (β-actin in our case), respectively. Error bars we had indicate RQ-MIN and RQ-MAX, which constitute the acceptable error for a 95% confidence limit according to Student's *t*-test.

Western blotting and immunoprecipitation. Cells were stimulated with Pam_3CSK_4 (100 ng ml^{-1}) or zymosan (100 μg ml^{-1}) and lysed with RIPA buffer and NP-40 (for immunoprecipitation) containing protease inhibitor cocktail (P8340, Sigma). Phosphatase inhibitor cocktail II was added for p-IκB detection. To examine the association between A20 and p62, NIH-3T3 cells were co-transfected with expression vectors for A20 and p62 (pcDNA5-A20-V5/His and pMI-p62-HA, respectively) by using Lipofectamine LTX (Invitrogen), as recommended by the supplier. The expression vectors for A20 and p62 were made in our laboratory, as fusions of the V5/His tag in the pcDNA5 backbone (Invitrogen) and the HA tag in the pMX backbone (Cosmobio), respectively. Immunoprecipitation was carried out by using Dynabeads Protein G Immunoprecipitation system (Invitrogen) with specific antibodies, followed by immunoblotting with indicated antibodies as recommended by the supplier. Signal intensity of blotting was determined by densitometry using the NIH-Image J software (http://rsbweb.nih.gov/ij/). Full blot data are shown in Supplementary Fig. 18.

Cell staining for confocal microscopy analyses. Cells were cultured on covered glasses. For staining, cells were washed with TBS containing 0.05% (vol/vol) Tween (TBS-T) and permeabilized with 0.25% (vol/vol) Triton in TBS, and then incubated with a primary antibody at 4 °C overnight, followed by staining with secondary antibody conjugated with fluorophore. Cells on cover glass were embedded to slide glass with mounting medium including 4′,6-diamidino-2-phenylindole (Prolong Gold, Invitrogen), and analysed for confocal microscopy. The Fiji software (http://fiji.sc/Fiji) was used to determine the intensity of fluorescence.

Statistical analysis. The two-tailed Student's *t*-test was used for statistical analyses of two-group comparisons. Multigroup comparisons were performed by a one-way analysis of variance followed by Tukey–Kramer multiple comparisons test.

References

1. Cemma, M., Kim, P. K. & Brumell, J. H. The ubiquitin-binding adaptor proteins p62/SQSTM1 and NDP52 are recruited independently to bacteria-associated microdomains to target Salmonella to the autophagy pathway. *Autophagy* **7,** 341–345 (2011).
2. Andrade, R. M., Wessendarp, M., Gubbels, M. J., Striepen, B. & Subauste, C. S. CD40 induces macrophage anti-*Toxoplasma gondii* activity by triggering autophagy-dependent fusion of pathogen-containing vacuoles and lysosomes. *J. Clin. Invest.* **116,** 2366–2377 (2006).
3. Orvedahl, A. *et al.* Autophagy protects against Sindbis virus infection of the central nervous system. *Cell Host Microbe* **7,** 115–127 (2010).
4. Shi, C. S. *et al.* Activation of autophagy by inflammatory signals limits IL-1beta production by targeting ubiquitinated inflammasomes for destruction. *Nat. Immunol.* **13,** 255–263 (2012).
5. Paul, S., Kashyap, A. K., Jia, W., He, Y. W. & Schaefer, B. C. Selective autophagy of the adaptor protein Bcl10 modulates T cell receptor activation of NF-kappaB. *Immunity* **36,** 947–958 (2012).

6. Castillo, E. F. *et al.* Autophagy protects against active tuberculosis by suppressing bacterial burden and inflammation. *Proc. Natl Acad. Sci. USA* **109,** E3168–E3176 (2012).
7. Ma, J., Becker, C., Lowell, C. A. & Underhill, D. M. Dectin-1-triggered recruitment of light chain 3 protein to phagosomes facilitates major histocompatibility complex class II presentation of fungal-derived antigens. *J. Biol. Chem.* **287,** 34149–34156 (2012).
8. Nicola, A. M. *et al.* Macrophage autophagy in immunity to *Cryptococcus neoformans* and *Candida albicans*. *Infect. Immun.* **80,** 3065–3076 (2012).
9. Smeekens, S. P. *et al.* Autophagy is redundant for the host defense against systemic *Candida albicans* infections. *Eur. J. Clin. Microbiol. Infect. Dis.* **33,** 711–722 (2014).
10. Rosentul, D. C. *et al.* Role of autophagy genetic variants for the risk of *Candida* infections. *Med. Mycol.* **52,** 333–341 (2014).
11. Lortholary, O. & Dupont, B. Antifungal prophylaxis during neutropenia and immunodeficiency. *Clin. Microbiol. Rev.* **10,** 477–504 (1997).
12. Koh, A. Y., Kohler, J. R., Coggshall, K. T., Van Rooijen, N. & Pier, G. B. Mucosal damage and neutropenia are required for *Candida albicans* dissemination. *PLoS Pathog.* **4,** e35 (2008).
13. Rubin-Bejerano, I., Fraser, I., Grisafi, P. & Fink, G. R. Phagocytosis by neutrophils induces an amino acid deprivation response in *Saccharomyces cerevisiae* and *Candida albicans*. *Proc. Natl Acad. Sci. USA* **100,** 11007–11012 (2003).
14. Van Eeden, S. F., Bicknell, S., Walker, B. A. & Hogg, J. C. Polymorphonuclear leukocytes L-selectin expression decreases as they age in circulation. *Am. J. Physiol.* **272,** H401–H408 (1997).
15. Cailhier, J. F. *et al.* Conditional macrophage ablation demonstrates that resident macrophages initiate acute peritoneal inflammation. *J. Immunol.* **174,** 2336–2342 (2005).
16. Sun, Y. *et al.* TLR4 and TLR5 on corneal macrophages regulate *Pseudomonas aeruginosa* keratitis by signaling through MyD88-dependent and -independent pathways. *J. Immunol.* **185,** 4272–4283 (2010).
17. Kubota, Y. *et al.* Role of alveolar macrophages in *Candida*-induced acute lung injury. *Clin. Diagn. Lab. Immunol.* **8,** 1258–1262 (2001).
18. Okabe, Y. & Medzhitov, R. Tissue-specific signals control reversible program of localization and functional polarization of macrophages. *Cell* **157,** 832–844 (2014).
19. Davies, L. C., Jenkins, S. J., Allen, J. E. & Taylor, P. R. Tissue-resident macrophages. *Nat. Immunol.* **14,** 986–995 (2013).
20. Schulz, C. *et al.* A lineage of myeloid cells independent of Myb and hematopoietic stem cells. *Science* **336,** 86–90 (2012).
21. Ghosn, E. E. *et al.* Two physically, functionally, and developmentally distinct peritoneal macrophage subsets. *Proc. Natl Acad. Sci. USA* **107,** 2568–2573 (2010).
22. Mordue, D. G. & Sibley, L. D. A novel population of Gr-1 + -activated macrophages induced during acute toxoplasmosis. *J. Leukoc. Biol.* **74,** 1015–1025 (2003).
23. Peters, W. *et al.* CCR2-dependent trafficking of F4/80dim macrophages and CD11cdim/intermediate dendritic cells is crucial for T cell recruitment to lungs infected with *Mycobacterium tuberculosis*. *J. Immunol.* **172,** 7647–7653 (2004).
24. Shembade, N. & Harhaj, E. W. Regulation of NF-kappaB signaling by the A20 deubiquitinase. *Cell Mol. Immunol.* **9,** 123–130 (2012).
25. Boone, D. L. *et al.* The ubiquitin-modifying enzyme A20 is required for termination of Toll-like receptor responses. *Nat. Immunol.* **5,** 1052–1060 (2004).
26. Lee, E. G. *et al.* Failure to regulate TNF-induced NF-kappaB and cell death responses in A20-deficient mice. *Science* **289,** 2350–2354 (2000).
27. Hammer, G. E. *et al.* Expression of A20 by dendritic cells preserves immune homeostasis and prevents colitis and spondyloarthritis. *Nat. Immunol.* **12,** 1184–1193 (2011).
28. Harhaj, E. W. & Dixit, V. M. Regulation of NF-kappaB by deubiquitinases. *Immunol. Rev.* **246,** 107–124 (2012).
29. Komatsu, M. *et al.* Impairment of starvation-induced and constitutive autophagy in Atg7-deficient mice. *J. Cell Biol.* **169,** 425–434 (2005).
30. Martinez, J. *et al.* Microtubule-associated protein 1 light chain 3 alpha (LC3)-associated phagocytosis is required for the efficient clearance of dead cells. *Proc. Natl Acad. Sci. USA* **108,** 17396–17401 (2011).
31. Fulurija, A., Ashman, R. B. & Papadimitriou, J. M. Neutrophil depletion increases susceptibility to systemic and vaginal candidiasis in mice, and reveals differences between brain and kidney in mechanisms of host resistance. *Microbiology* **142,** 3487–3496 (1996).
32. Balish, E. *et al.* Mucosal and systemic candidiasis in IL-8Rh-/- BALB/c mice. *J. Leukoc. Biol.* **66,** 144–150 (1999).
33. Cravens, P. D. & Lipsky, P. E. Dendritic cells, chemokine receptors and autoimmune inflammatory diseases. *Immunol. Cell Biol.* **80,** 497–505 (2002).
34. Criollo, A. *et al.* Autophagy is required for the activation of NFkappaB. *Cell Cycle* **11,** 194–199 (2012).
35. Li, M. *et al.* An essential role of the NF-kappa B/Toll-like receptor pathway in induction of inflammatory and tissue-repair gene expression by necrotic cells. *J. Immunol.* **166,** 7128–7135 (2001).
36. Grove, M. & Plumb, M. C/EBP, NF-kappa B, and c-Ets family members and transcriptional regulation of the cell-specific and inducible macrophage inflammatory protein 1 alpha immediate-early gene. *Mol. Cell. Biol.* **13,** 5276–5289 (1993).
37. Zhang, Z. *et al.* CCAAT/enhancer-binding protein beta and NF-kappaB mediate high level expression of chemokine genes CCL3 and CCL4 by human chondrocytes in response to IL-1beta. *J. Biol. Chem.* **285,** 33092–33103 (2010).
38. Akira, S., Takeda, K. & Kaisho, T. Toll-like receptors: critical proteins linking innate and acquired immunity. *Nat. Immunol.* **2,** 675–680 (2001).
39. Skaug, B. *et al.* Direct, noncatalytic mechanism of IKK inhibition by A20. *Mol. Cell* **44,** 559–571 (2011).
40. Li, L. *et al.* Localization of A20 to a lysosome-associated compartment and its role in NFkappaB signaling. *Biochim. Biophys. Acta* **1783,** 1140–1149 2008.
41. Pankiv, S. *et al.* p62/SQSTM1 binds directly to Atg8/LC3 to facilitate degradation of ubiquitinated protein aggregates by autophagy. *J. Biol. Chem.* **282,** 24131–24145 (2007).
42. Paludan, C. *et al.* Endogenous MHC class II processing of a viral nuclear antigen after autophagy. *Science* **307,** 593–596 (2005).
43. English, L. *et al.* Autophagy enhances the presentation of endogenous viral antigens on MHC class I molecules during HSV-1 infection. *Nat. Immunol.* **10,** 480–487 (2009).
44. Martinet, W., Schrijvers, D. M., Timmermans, J. P., Herman, A. G. & De Meyer, G. R. Phagocytosis of bacteria is enhanced in macrophages undergoing nutrient deprivation. *FEBS J.* **276,** 2227–2240 (2009).
45. Brothers, K. M. *et al.* NADPH oxidase-driven phagocyte recruitment controls *Candida albicans* filamentous growth and prevents mortality. *PLoS Pathog.* **9,** e1003634 (2013).
46. Tam, J. M. *et al.* Dectin-1-dependent LC3 recruitment to phagosomes enhances fungicidal activity in macrophages. *J. Infect. Dis.* **210,** 1844–1854 (2014).
47. Saijo, S. *et al.* Dectin-1 is required for host defense against *Pneumocystis carinii* but not against *Candida albicans*. *Nat. Immunol.* **8,** 39–46 (2007).
48. Taylor, P. R. *et al.* Dectin-1 is required for beta-glucan recognition and control of fungal infection. *Nat. Immunol.* **8,** 31–38 (2007).
49. Shi, C. S. & Kehrl, J. H. TRAF6 and A20 regulate lysine 63-linked ubiquitination of Beclin-1 to control TLR4-induced autophagy. *Sci. Signal* **3,** ra42 (2010).
50. Maelfait, J. *et al.* A20 (Tnfaip3) deficiency in myeloid cells protects against influenza A virus infection. *PLoS Pathog.* **8,** e1002570 (2012).
51. Jia, W., Pua, H. H., Li, Q. J. & He, Y. W. Autophagy regulates endoplasmic reticulum homeostasis and calcium mobilization in T lymphocytes. *J. Immunol.* **186,** 1564–1574 (2011).
52. Tavares, R. M. *et al.* The ubiquitin modifying enzyme A20 restricts B cell survival and prevents autoimmunity. *Immunity* **33,** 181–191 (2010).
53. Harada, H. *et al.* Deficiency of p62/Sequestosome 1 causes hyperphagia due to leptin resistance in the brain. *J. Neurosci.* **33,** 14767–14777 (2013).
54. Inoue, M. *et al.* T cells down-regulate macrophage TNF production by IRAK1-mediated IL-10 expression and control innate hyperinflammation. *Proc. Natl Acad. Sci. USA* **111,** 5295–5300 (2014).

Acknowledgements

We thank Drs W. Jia, M. He and Irm I. McLeod for their help setting up the *Atg7*$^{fl/fl}$ *LysM*$^{cre/+}$ mouse line and experimental techniques related to autophagy; Dr T. Yanagawa (University of Tsukuba, Japan) for providing *p62*$^{fl/fl}$LysM-Cre mice and Dr J. Heitman (Department of Molecular Genetics and Microbiology, Duke University) for providing *C. albicans*. This work was supported by the National Institutes of Health (R01AI088100 to M.L.S.) and by the Uehara Memorial Foundation Fellowship (to M.K.).

Author contributions

M.K. performed the experiments with assistance from M.I. and K.D. Y.-W.H. and G.H. participated in data interpretation and critical discussions. M.K. and M.L.S. designed experiments, analysed data and wrote the manuscript.

Additional information

Competing financial interests: The authors declare no competing financial interests.

Reprints and permission information is available online at http://npg.nature.com/reprintsandpermissions/

How to cite this article: Kanayama, M. *et al.* Autophagy enhances NFκB activity in specific tissue macrophages by sequestering A20 to boost antifungal immunity. *Nat. Commun.* 6:5779 doi: 10.1038/ncomms6779 (2015).